ISSN 1063-7737, Astronomy Letters, 2007, Vol. 33, No. 3, pp. 192–202. © Pleiades Publishing, Inc., 2007.
Original Russian Text © G.P. Chernov, A.A. Stanislavsky, A.A. Konovalenko, E.P. Abranin, V.V. Dorovsky, 2007, published in Pis'ma v Astronomicheskiĭ Zhurnal, 2007, Vol. 33, No. 3, pp. 221–232.

Fine Structure of Decametric Type II Radio Bursts

G. P. Chernov[1*], A. A. Stanislavsky[2], A. A. Konovalenko[2], E. P. Abranin[2], V. V. Dorovsky[2], and H. O. Rucker[3]

[1] *Pushkov Institute of Terrestrial Magnetism, Ionosphere, and Radiowave Propagation (IZMIRAN), Russian Academy of Sciences, Troitsk, Moscow oblast, 142190 Russia*

[2] *Institute of Radio Astronomy, National Academy of Science of Ukraine, Krasnoznamennaya ul. 35, Kharkov, 61002 Ukraine*

[3] *Space Research Institute, Austrian Academy of Sciences, Austria*

Received June 24, 2006

Abstract—We have performed a comparative analysis of the fine structure of two decametric type II bursts observed on July 17 and August 16, 2002, with the 1024-channel spectrograph of the UTR-2 radio telescope in the frequency range 18.5–29.5 MHz and with the IZMIRAN spectrograph in the frequency range 25–270 MHz. The August 16 burst was weak, ~2–5 s.f.u., but exhibited an unusual fine structure in the form of broadband fibers ($\Delta f_e > 250$–500 kHz) that drifted at a rate characteristic of type II bursts and consisted of regular narrow-band fibers ($\Delta f_e > 50$–90 kHz at 24 MHz) resembling a rope of fibers. The July 17 burst was three orders of magnitude more intense (up to 4500 s.f.u. at 20 MHz) and included a similar fiber structure. The narrow fibers were irregular and shorter in duration. They differed from an ordinary rope of fibers by the absence of absorption from the low-frequency edge and by slow frequency drift (slower than that of a type II burst). Both type II bursts were also observed in interplanetary space in the WIND/WAVES RAD2 spectra, but without any direct continuation. Analysis of the corresponding coronal mass ejections (CMEs) based on SOHO/LASCO C2 data has shown that the radio source of the type II burst detected on August 16 with UTR-2 was located between the narrow CME and the shock front trailing behind that was catching up with the CME. The July 17 type II fiber burst also occurred at the time when the shock front was catching up with the CME. Under such conditions, it would be natural to assume that the emission from large fibers is related to the passage of the shock front through narrow inhomogeneities in the CME tail. Resonant transition radiation may be the main radio emission mechanism. Both events are characterized by the possible generation of whistlers between the leading CME edge and the shock front. The whistlers excited at shock fronts manifest themselves only against the background of enhanced emission from large fibers (similar to the continuum modulation in type IV bursts). The reduction in whistler group velocity inside inhomogeneities to 760 km s^{-1} may be responsible for the unusually low drift rate of the narrow fibers. The magnetic field inside inhomogeneities determined from fiber parameters at 24 MHz is ~0.9 G, while the density should be increased by at least a factor of 2.

PACS numbers : 96.60.Hv; 96.60.ph
DOI: 10.1134/S1063773707030061

Key words: *Sun, radio bursts, flares, fibers, plasma waves, whistlers.*

INTRODUCTION

Solar type II radio bursts attract the rapt attention of researchers, because they occur during large flares and are produced by shock waves that usually escape into interplanetary space, reaching the Earth's orbit. However, in the decametric wavelength range (10–30 MHz), a gap in studies related to the absence of appropriate radio telescopes and adequate recording equipment has been felt until recently. The first reports on the analysis of type II radio bursts in the decametric range (Melnik et al. 2004) and a fine structure in the form of pair bursts (Melnik et al. 2005) appeared after the UTR-2 radio telescope had been upgraded.

However, the analysis of the fine structure has so far concerned only features like a herringbone structure and an irregular patchy structure in the shape of rapidly drifting short-duration spikes. Even these first results point to a great variety of features in the structure inherent in decametric type II bursts. This problem requires separate attention in studies.

In this paper, the fine structure of type II bursts

*E-mail: gchernov@izmiran.rssi.ru

in the form of drifting fibers observed with the digital 1024-channel spectrograph of the UTR-2 radio telescope with a time resolution of 100 ms in the frequency range 17.5–29.5 MHz is analyzed in detail for the first time. Analysis of this fine structure is the key to understanding the plasma processes high in the corona and using all of the currently available WIND, SOHO, and TRACE data on flares in other wavelength ranges allows additional information about the propagation of shock waves escaping into interplanetary space to be obtained.

The stripes in emission and absorption against the continuum background of solar type II–IV radio bursts in the metric range are traditionally subdivided into two types: a zebra pattern (ZP) and intermediate drift bursts (IDB or fiber bursts). They are usually observed in a pulsating regime and against the background of fast broadband radio emission pulsations. They have long been studied and classified in atlases (Slottje 1981) and monographs (Kruger 1979). Here, our objective is to compare a similar fine structure in the decametric range with available data in the metric wavelength range. The first evidence for the existence of unusual narrow-band fibers in the frequency range 25–50 MHz appeared long ago (Thompson and Maxwell 1962). However, no detailed up-to-date studies have been performed so far.

OBSERVATIONS

A General Description of the August 16, 2002 Event

Several type II radio bursts, at least two bursts in the metric range and two interplanetary bursts (below 14 MHz on the WIND/WAVE spacecraft), were observed after a small M2.4/SF flare at the western limb of the solar disk (active region AR 0061, N07W83) on August 16 from 05:46 until 06:37 UT. According to the Culgoora Observatory data, the first type II burst in the frequency range 180–57 MHz began at 05:52 UT (http://www.ips.oz.au/ Solar/2/6/1). No direct continuation of this burst is found in the WIND/WAVES/RAD2 spectrum, but four drifting stripes forming pairwise harmonic frequency structures (characteristic of type II bursts) appeared after about 06:15 UT at frequencies <3.5 MHz. This interplanetary burst is shown in Fig. 1a against the background of numerous type III bursts. A continuum then appeared in the Culgoora spectrum in the metric range. Its brightest part exhibited a drift to high frequencies after 06:07 UT. Subsequently, a continuum slowly drifting to low frequencies (to the end of the spectrum at 57 MHz) followed at 06:17. Starting from the beginning of UTR-2 observations, at 06:33:23 UT, this slowly drifting continuum was recorded at frequencies 12.5–19 MHz until 06:40:00 UT. Its direct continuation appeared in the RAD2 spectrum at 06:30 UT. The drifting continua closely coincide with the IZMIRAN 25–270 MHz spectra.

In the RAD2 spectrum, this continuum continued (again with a gap over the range) in the form of patches of the type II burst at 07:22 UT. The type II burst with a fine structure observed on UTR-2 after 07:20 UT in the frequency range 18.5–29.5 MHz and shown in Fig. 1b was weak in intensity and had a low frequency, since it was not detected at frequencies above 30 MHz with the IZMIRAN spectrograph whose sensitivity is three orders of magnitude lower than that of UTR-2. A preliminary description of this spectrum was given by Melnik et al. (2004).

Two coronal mass ejections (CMEs) are pointed out in the catalog of the SOHO/LASCO C2 coronagraph. The first, slow CME propagated with a velocity of 493 km s^{-1} starting from 05:30 UT. It preceded the shock wave responsible for the metric type II burst at 05:52 UT (the shock wave propagated much lower in the corona). The second, more intense and fast CME appeared on C2 at 06:06 UT; it propagated with a velocity of 1378 km s^{-1} and caught up with (and absorbed by) the first CME approximately at 06:40 UT. The intersection of their trajectories in the height–time diagram is shown in Fig. 2. After the absorption of the slow CME, its trajectory is extended by the dotted line; it was no longer distinguished in the C2 images.

To clearly understand the relationship between the shock waves (type II bursts, after 07:20 UT) and the CMEs, we will use the lucky coincidence of the C2 coronagraph heights ($2–5R_\odot$) with the range of heights ($1.8–6R_\odot$) from which the radio emission in the WIND RAD2 frequency range (1–14 MHz) originates. Such height estimates can be easily obtained using a model electron density (plasma frequency) distribution in interplanetary space calculated by Leblanc et al. (1998), which agrees well with the Newkirk model above an active region in the corona.

It is clear from the aforesaid that the decametric type II burst whose features are presented in Fig. 1a is in no way associated with the continuum burst that appeared in the RAD2 spectrum at 06:30 UT and that continued in the form of patches until 07:30 UT.

The flare evolution can be seen in the SOHO/EIT images in the 195 Å line shown for four consecutive times in Fig. 3. The left frame shows the ejection at 05:48 UT with which the appearance of the first type II burst at 05:52 UT at 180 MHz (Culgoora spectrum) is associated. The new flare loops forming two arcades, whose intersection looks like an X point of magnetic reconnection in the succeeding frames,

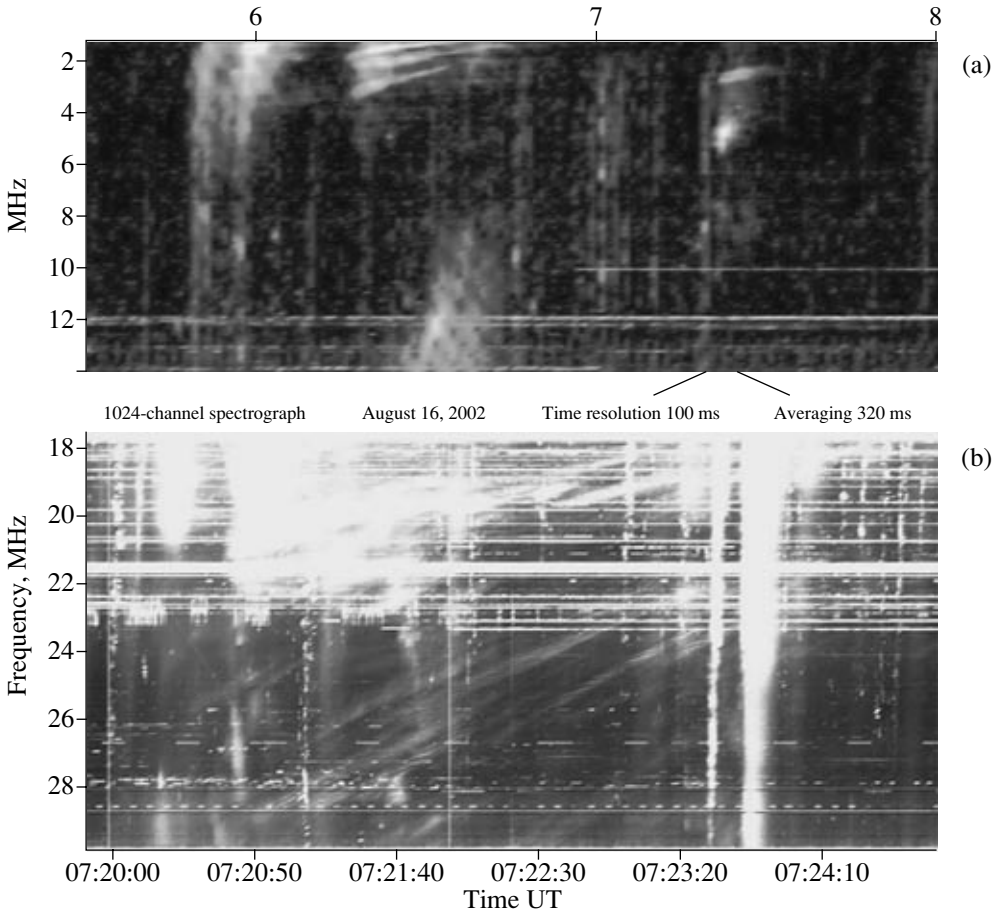

Fig. 1. (a) WIND/WAVE RAD2 spectrum in the frequency range 1–14 MHz (http://lep694.gsfc.nasa.gov/waves/waves.html) containing three different type II bursts against the background of numerous type III bursts. (b) UTR-2 spectrum in the frequency range 18.5–29.5 MHz showing an unusual fine structure of broadband fibers with a superfine structure in the form of narrow-band fibers.

began to rise at 07:13 UT. The subsequent growth and rise of the flare loops after another ejection are shown in the succeeding frames. The dynamics of the loops with bright flare kernels at the loop intersection lasted for more than an hour. If, however, we turn to the LASCO C2 images, then we will detect this new narrow ejection marked by the arrow in the right frame of Fig. 4. Thus, the flare process shown in Fig. 3 was probably accompanied by simultaneous reconnection high in the corona with the formation of magnetic islands and a new narrow CME. In Fig. 2, this new CME (not included in the catalog) is marked by the thin dotted line between 06:50 and 07:20 UT. It can only be assumed that the ejection shown in the frame in Fig. 3 at 07:13 UT could produce a piston shock wave propagating along the tail of the narrow CME and that it is this shock wave that was the source of the decametric type II burst on the UTR-2 records that had a small continuation in interplanetary space in the form of several patches in the RAD2 spectrum after 07:23 UT (Fig. 1a). According to Fig. 2, the leading edge of this new narrow CME at the time when the fine structure appeared had already gone far outside the range of heights corresponding to the UTR-2 frequency range (18–30 MHz) marked by the lower thick dotted line. Thus, the radio source of the fine structure in the UTR-2 spectrum could be in the tail of the narrow CME at the shock front. Comparison of the RAD2 spectrum at the time when the continuum burst appeared at 06:25 with the left LASCO C2 image shows that the leading edge of the brightest ejection in the tail of the main CME is located at the heights ($\sim 1.8 R_\odot$) corresponding to a frequency of 14 MHz.

The Radio Burst Fine Structure in the 18.5–29.5 MHz Frequency Band

The radio bursts in Fig. 1b are the various elements of the weak type II burst and the numerous type III bursts drifting almost through the entire range. The fibers exhibit the most unusual fine

structure: irregular broadband (with different instantaneous widths $\Delta f_e > 250$–500 kHz) fibers with a superfine structure in the form of narrow-band fibers (with band widths $\Delta f_e > 50$–90 kHz). The frequency separation between the latter rarely exceeds 50 kHz. Large fibers have a frequency drift rate $df/dt > -0.0365$ MHz s^{-1} characteristic of type II bursts at these frequencies, while small fibers (in large ones) have a frequency drift rate from a value almost equal to the drift rate of large fibers (parallel fibers at 07:22:30-50 UT in the largest fiber) to a minimum (on average) value, > -0.019 MHz s^{-1}. All large fibers have similar frequency drift rates, but they are spread randomly over the spectrum, with some of them exhibiting virtually no superfine structure. Narrow-band fibers are observed only in large fibers. Five narrow parallel fibers forming a so-called rope of fibers well known in the metric wavelength range (Chernov 1997) can be simultaneously distinguished in the largest fiber. In the event under consideration, the narrow fibers differ from a rope of fibers only by a slower frequency drift.

Note the following important property of this event: it was a limb one and very weak in intensity: the flux density in weak fibers was, on average, 2–3 s.f.u. (1 s.f.u. $= 10^{-22}$ W m^{-2} Hz^{-1}), while for the two successive type III bursts after 07:23:20 UT (the brightest ones in the spectrum in Fig. 1b) at 20 MHz the flux density was 24 s.f.u. The flux densities are presented in Fig. 5 at two frequencies together with a magnified fragment of the fiber spectrum. The fiber profile times are marked by the straight line segments under the profiles. The profiles reveal no clear absorption of the background burst between the fibers, i.e., there is no low-frequency absorption characteristic of intermediate drift fibers (IDB fibers or a rope of fibers).

Some of the type III bursts also exhibit a fine structure in the form of stripes or patches; the stripes occasionally drift with the same rate as the narrow fibers, when they are near the fibers, for example, at 07:21:08 UT. The spectrum is further complicated by the presence of reverse-drifting type III bursts, which also contain stripes with a drift similar to that of the fibers (e.g., at 07:21:40 and 07:23:20 UT).

We see a clear analogy of the fiber structure in this event with that at close frequencies in the May 2, 1998 event described by Chernov (2004), although the latter was much more intense and had a larger scale. The parameters of both large and small fibers are approximately identical and the small fibers in a large fiber (rope) then also drifted with a lower rate. The main difference of the May 2, 1998 event was that the large fiber was then a single and longer-lived one, while the small fibers appeared throughout

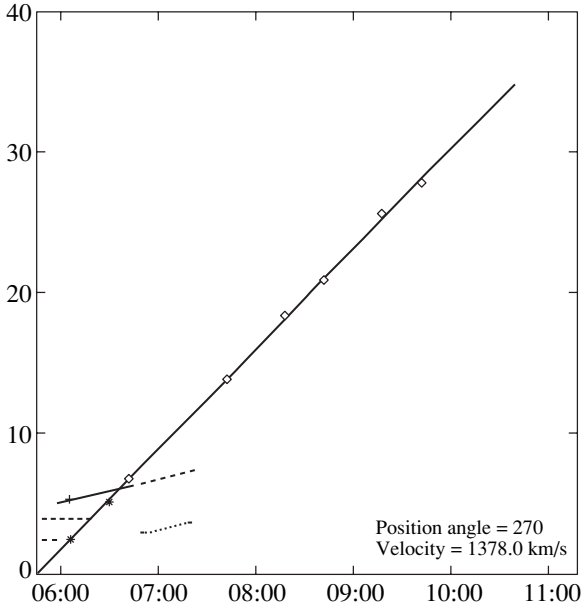

Fig. 2. Height–time diagram for several CMEs observed on August 16, 2002. The trajectory of an intense CME at 06:06 UT (from the LASCO catalog, http://cdaw.gsfc.nasa.gov/CME_list/) is shown along with the trajectory of a slow CME at 05:30 UT absorbed by the intense CME and the trajectory of a new small CME at 06:50 UT. The lower thick dotted line at a height of $1.4R_\odot$ corresponds to the middle point of the UTR-2 range ($\sim$23 MHz), while the upper thick dotted line at a height of $3R_\odot$ corresponds to the frequency of 3.7 MHz at which the interplanetary type II burst began at 06:15 UT.

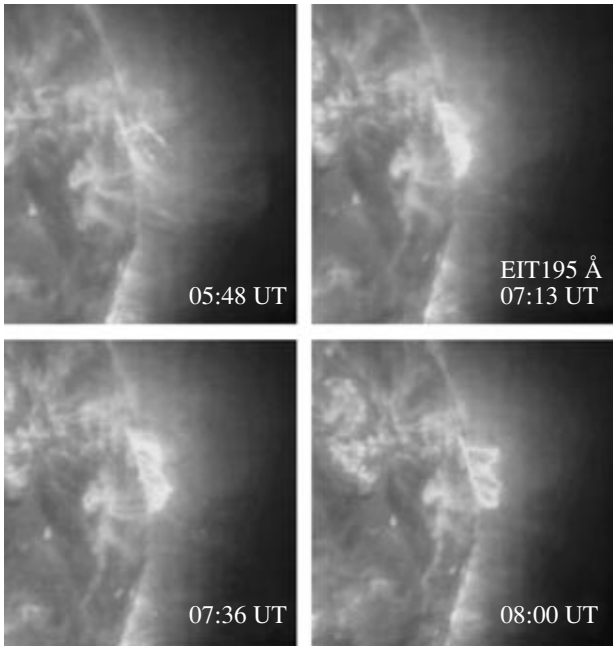

Fig. 3. Four consecutive development times of the August 16, 2002 flare in the limb active region AR10061 in the 195 Å SOHO/EIT line.

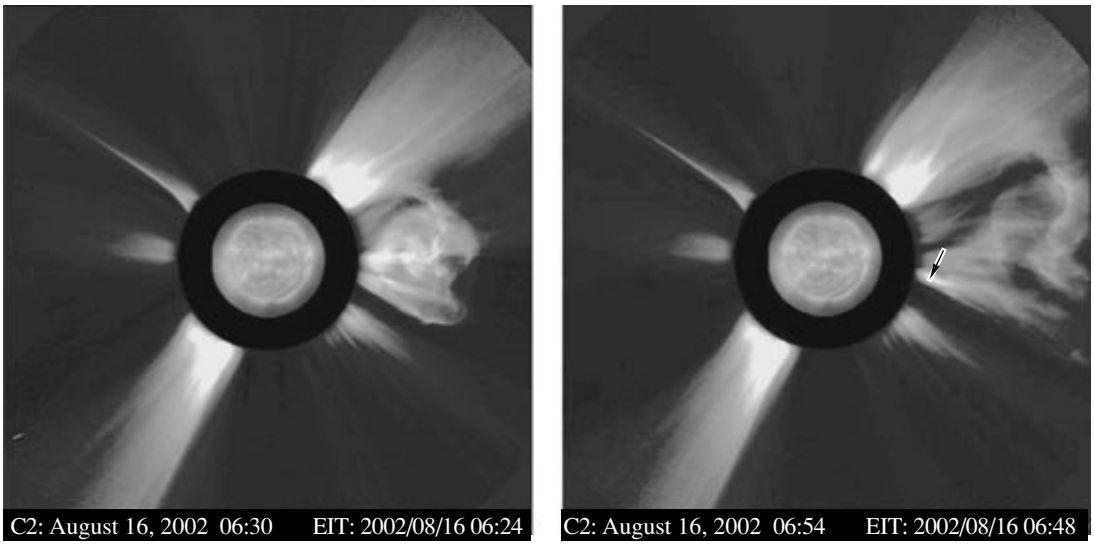

Fig. 4. Two images from the LASCO C2 video clip. In the left image, the new bright ejections behind the leading CME edge coincide in time and position with the appearance of a drifting continuum at the high-frequency edge of the RAD2 spectrum; the narrow tortuous fronts at the leading edge are probably associated with the two shock waves generated by the collision of two CMEs. In the right image, the arrow indicates the new narrow CME (not included in the catalog) that appeared in the tail of the preceding CME and that coincides with several new patches in the RAD2 spectrum in the 7–10 MHz frequency band.

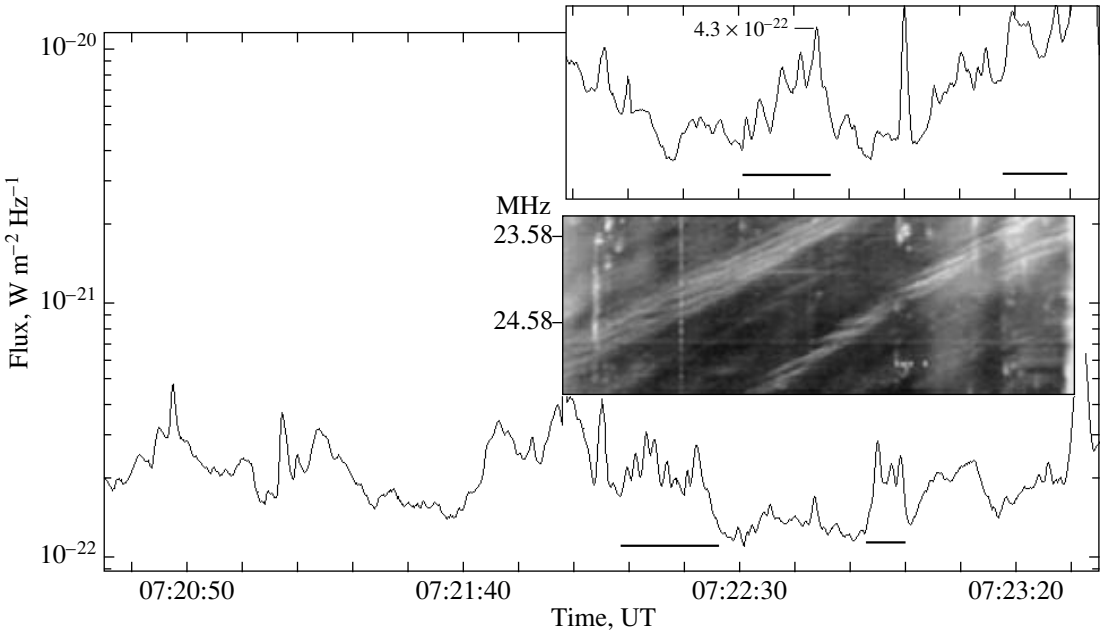

Fig. 5. Profiles of the 1024-channel spectrograph at two frequencies combined with the dynamic UTR-2 spectrum. The times of the fiber profiles are marked by the straight line segments under the profiles. The profile for a frequency of 23.58 MHz is shown at the top.

the spectrum, grouping only occasionally into large ropes. The May 2, 1998 event in combination with the WIND/WAVE data is described in more detail in Chernov et al. (2006).

Thus, narrow fibers are the fine structure of large fibers and, although they are similar in overall spectral shape to a rope of fibers, no intermediate drift rate is reached in these two events. However, as was shown for the May 2, 1998 event, a slow drift is determined by a reduced whistler group velocity at the shock front (Chernov et al. 2006). The absence of low-frequency absorption is often also characteristic of ordinary fibers in the metric range.

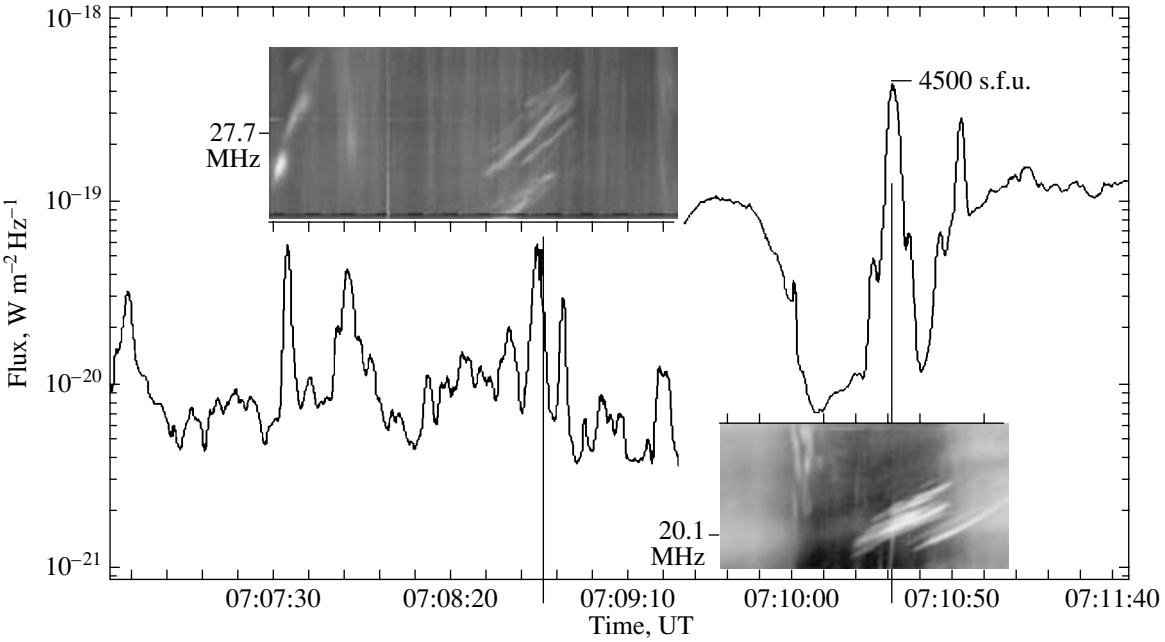

Fig. 6. Fiber profiles at two frequencies, 27.7 and 20.1 MHz, combined with the spectra on the same scale in the July 17, 2002 event. The peak flux at 20.1 MHz reached 4500 s.f.u. The width of the spectra is ~3.7 MHz.

A General Description of the July 17, 2002 Event

The July 17, 2002 event is of considerable interest for comparison with the August 16, 2002 event described above, since it had a similar fine structure of radio emission (fibers), but was three orders of magnitude more intense (cf. Figs. 5 and 6), while the M8.5 1B flare occurred near the disk center (N21W17) in the huge active region AR 0030.

The type II burst was observed only at low frequencies, 17.7–45 MHz, and was weaker than the intense groups of type III bursts (both before and after the type II burst (the lower IZMIRAN spectrum in Fig. 7). The fragment of the type II burst from UTR-2 measurements in the 17.5–29.5 MHz frequency band (the middle spectrum in Fig. 7) contains two groups of fibers. The fiber frequency drift is approximately equal to that of the type II burst at 07:08:30 UT and is appreciably slower than that at 07:10:40 UT.

The type II burst in the WIND/WAVES RAD2 records is not its direct continuation: instead of ~07:10, it appeared only at 07:30 at 3.8 MHz, i.e., with a frequency gap (the upper spectrum in Fig. 7). However, the two bursts fall on the trajectory of the CME in time and source height (its velocity is 716 km s^{-1}) appeared on LASCO C2 only at 07:31 UT. The flare detected in the EIT 195 Å line is present only at 07:13 (this time is close to the maximum). Two ejections at 07:04 going away from a two-ribbon arcade of bright loops are seen in the (TRACE) images of the flare in the 1600 Å line (Fig. 8). The emission in the 1600 Å band (the UV line and the continuum emission) reflects the processes in the transition region at a temperature of ~10^5 K). The subsequent motion of the ejections is traceable at 07:06 in the 284 Å SOHO/EIT line, which reflects the processes in the hotter (up to 3×10^6 K) flare loops higher in the corona. The onset of the type II burst coincides with the continuation of this ejection into the corona. Fitting the CME trajectory (a height–time dependence similar to Fig. 2) shows that the CME was born earlier than this ejection, at ~06:30 UT. It would be natural to associate the appearance of a shock wave with this ejection; its velocity determined from the frequency drift of the type II burst between 45 and 30 MHz ($df/dt \sim -0.1$ MHz s^{-1}) is considerably higher than the CME velocity, ~1200 km s^{-1}. Since the radio sources fall on the CME trajectory (according to the density model by Leblanc et al. (1998)), this type II fiber burst occurred at the time when the shock caught up with the CME. This is in good agreement with the previous assumption about the formation of a fine structure as the shock wave propagates in the CME tail. After the collision of the shock wave with the CME, the shock front velocity became almost equal to the CME velocity ($V \sim 650$ km s^{-1}, as derived from the burst frequency drift rate on RAD2 between 3.3 and 2 MHz).

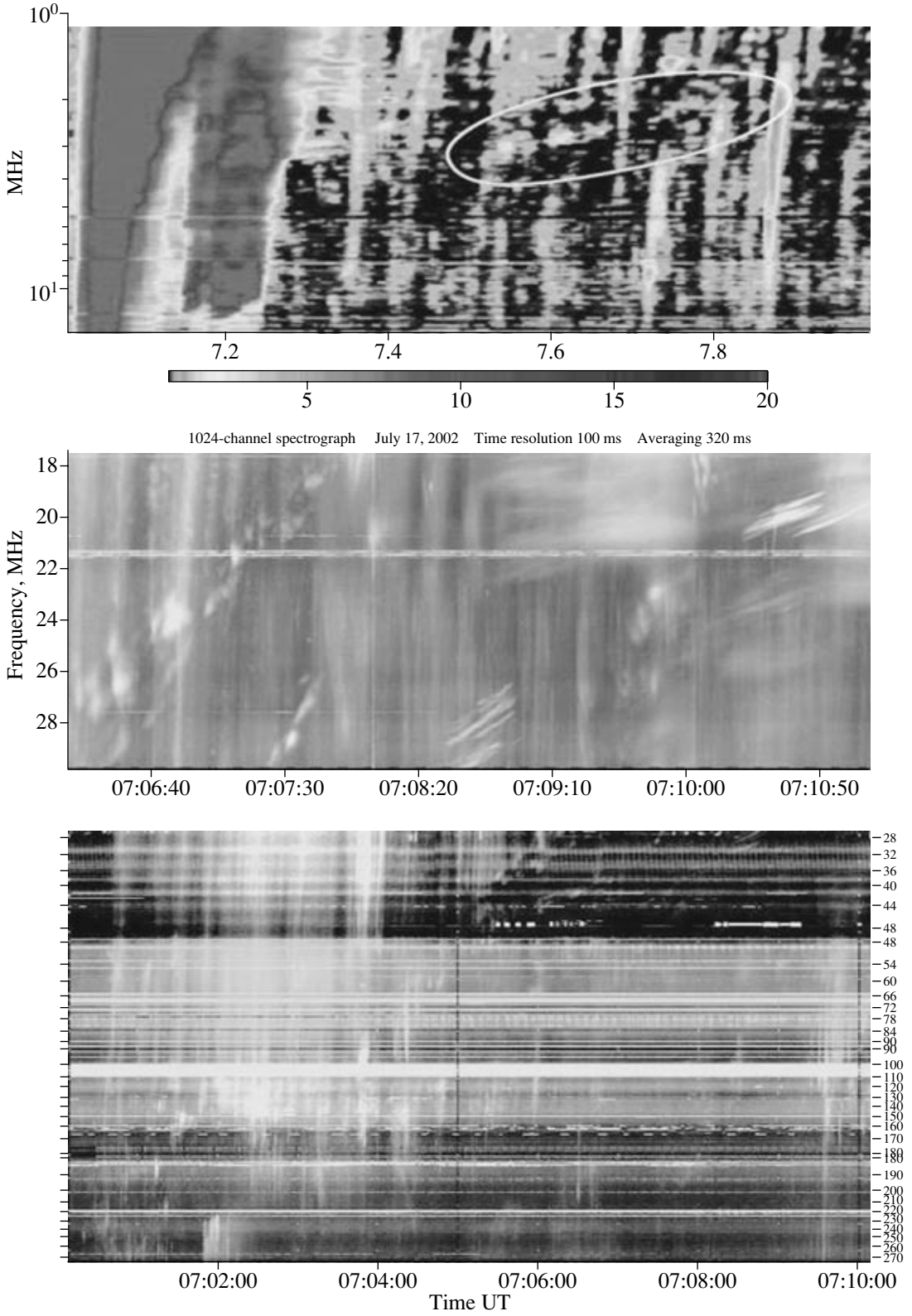

Fig. 7. Combined spectrum of the July 17, 2002 event. The IZMIRAN spectrum in the metric range (26–270 MHz) is shown in the lower panel. The UTR-2 spectrum in the frequency range 18.5–29.5 MHz exhibiting patches of the type II burst and three groups of unusual fibers is shown in the middle panel; their frequency drift rate is lower than the mean drift rate of the type II burst and decreases with time and frequency. The 1–14 MHz (WIND/WAVE RAD2) spectrum containing a weak type II burst (in the oval) against the background of numerous type III bursts is shown in the upper panel.

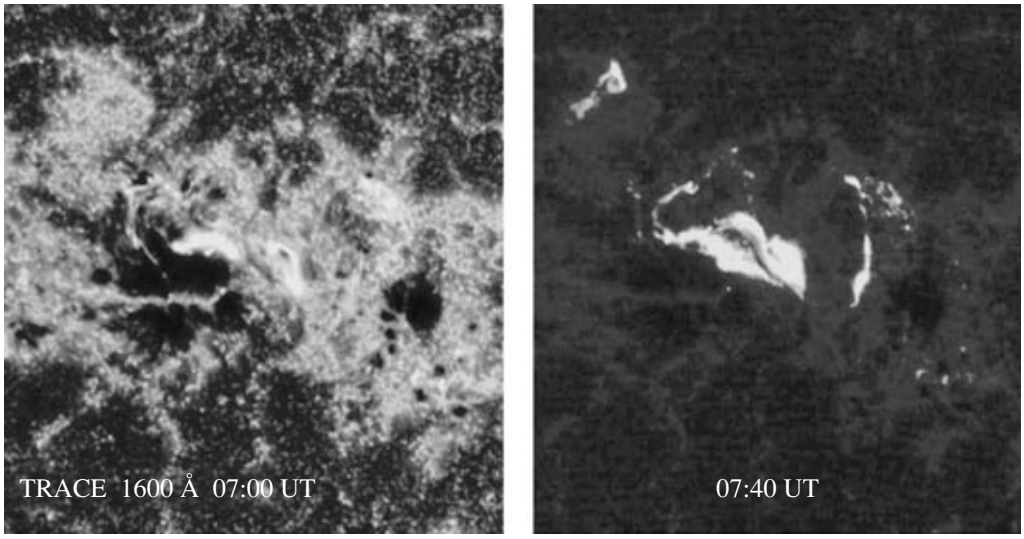

Fig. 8. Evolution of the July 17, 2002 flare in the 1600 Å (TRACE) line: the onset time of the flare in the form of two growing loops is shown on the left; a time close to the maximum with two ejections is shown on the right.

The Fine Structure of the July 17, 2002 Radio Burst in the 18.5–29.5 MHz Frequency Band

Note that the fine structure in the form of fibers differs from the August 16, 2002 event by a shorter duration, ~20–30 s. Instead of large fibers, they form two groups. The diffuse group between 22–24 MHz under the intense second group can also be noted. Apart from the type III bursts, the spectrum simultaneously exhibits a number of other bursts: short-lived forward and reverse drift bursts long-lived diffuse bursts. Moreover, the groups of fibers are observed against the background of diffuse emission. Note the following important fact: the fibers in the 27–29.5 MHz band (as well as other features) closely coincide in time in the UTR-2 and IZMIRAN spectra (Fig. 7), suggesting that the fine structure is solar in origin. The fibers in groups follow irregularly both in time and in frequency. All of the fibers also differ in band width; they appear as individual bursts. The band width Δf_e changes from its minimum value, >0.028 MHz, to its maximum value, >0.1 MHz. The frequency drift rate of the fibers in the first group is -0.08 MHz s^{-1}, i.e., it is lower than that of the patchy type II stripe, where $df/dt > -0.11$ MHz s^{-1}. In the second group, the frequency drift rate is the same as that for the large fibers on August 16, 2002, $df/dt > -0.036$ MHz s^{-1}.

The fibers do not exhibit a clear low-frequency absorption either. The large dips between the fibers of the second group (Fig. 6) are most likely related to the absence of diffuse emission at these times in a broad frequency band and not directly to the fibers.

Thus, the main difference between the fibers in the weak and strong events manifested itself mainly in the breakdown of a strict fiber periodicity in the strong event.

The low intensity of the August 16, 2002 burst is most likely related to the directivity of the radio emission from the limb source, since the flares differ little in X-ray importance.

DISCUSSION

The August 16, 2002 Burst

Recall that we determined the position of the type II radio burst source between the narrow CME and the shock front trailing behind that was catching up with the CME. In terms of the plasma mechanism and the model of density N_e in interplanetary space calculated by Leblanc et al. (1998), the plasma frequency gradient is $df/dr > -4.79 \times 10^{-5}$ MHz km^{-1} (in the frequency range 10–40 MHz). The shock front velocity

$$V \approx 2\frac{df/dt}{f}\frac{N_e}{dN_e/dr} = \frac{df/dt}{df/dr}, \qquad (1)$$

determined from the frequency drift $df/dt = -0.04$ MHz s^{-1} is 830 km s^{-1}.

The minimum drift of the narrow fibers was ~ -0.02 MHz s^{-1}. The smooth increase in drift rate points to a change in the agent velocity from 400 to 830 km s^{-1}.

In the May 2, 1998 event, the source was located between two diverging shock fronts also in the CME tail. The large fibers can be explained most naturally by the emission excited when the shock front passes along the elongated narrow streamers, the inhomogeneities remaining behind the leading CME edge.

The instantaneous band width of the large fibers, $\Delta f_e > 250-500$ kHz, allows the inhomogeneity thickness in the propagation direction of the shock front, $\Delta f_e/(df/dr)$, to be estimated. The maximum thickness can be ~10 000 km.

The density inside the streamers can be twice the ambient plasma density and we see the maximum emission only from the streamers (Vrsnak et al. 2004). The presence of fast particles accelerated at the shock front may be considered obvious, given the appearance of oppositely drifting type III bursts in our spectrum and the numerous ordinary type III bursts at lower frequencies (Fig. 1a), many of which are the herringbone structure of a type II burst. Therefore, it would be natural to assume that the enhanced radio emission from large fibers is the transition radiation, the radiation from fast particles at the boundary between two media with different refractive indices (Fleishman et al. 2001). The transition radiation has already been suggested to explain the continuum in the zebra-pattern sources in the metric range by LaBelle et al. (2003). In interplanetary space, it can be much more efficient, since the transition radiation flux is proportional to the square of the density contrast in percent $(\rho\ \%)^2$ (Eq. (15) in LaBelle et al. (2003)). Whereas in the metric range ρ can reach only a few percent, the density contrast in the streamers in the CME tail can be ~100%. In addition, the resonant radiation increases sharply if the wavelength becomes equal to the density inhomogeneity sizes (the so-called resonant transition radiation (Nita et al. 2005). The satisfaction of this condition is much more likely in the CME tail at large heights.

In the August 16, 2002 event, we estimated the shock velocity, ~830 km s^{-1}, at a frequency of 24 MHz (in the model by Leblanc et al. (1998)). Our estimates of the magnetic field strength, $B \sim 0.9$ G (see below), allow the Alfvén velocity, $V_A \sim 730$ km s^{-1}, and the Mach number, ~1.14, to be estimated at the boundary of the critical value for the emission of plasma waves at the fronts of collisionless type II shock waves in the upper corona (Fomichev 1986). The shock wave in specific segments of its path can be both quasi-longitudinal and quasi-transverse with respect to the background magnetic field. However, particles are known to be accelerated at the shock front in both cases (Zaitsev and Ledenev 1976; Holman and Pesses 1983).

Fast particles accelerated at the shock front can be captured into a small trap between the leading CME edge and the shock front. The electrons reflected from the shock front form a loss-cone velocity distribution unstable for the generation of whistlers. Therefore, even one particle beam will lead to periodic whistler excitation through bounce motions in such a trap. According to Fig. 2, the separation between the leading CME edge and the presumed shock front (the position of the plasma level corresponding to the onset of emission at 30 MHz) is ~$1R_\odot$ and fast particles with velocities ~10^{10} cm s^{-1} characteristic of type III bursts provide a whistler excitation period of ~7 s. In the spectrum of Fig. 1b, this proves to be the maximum period between narrow fibers at the same frequency. Shorter periods (2–3 s at 07:22:30 UT) result from the reflection of two beams from both mirrors.

Thus, we can explain the presence of narrow fibers only in large fibers and it is related to a modulation of the continuum emission from large fibers by whistlers as a result of their merging with plasma waves (this is the widely known formation mechanism of fiber bursts; see Kuijpers 1975; Chernov 1976). In this model, we can estimate the magnetic field inside an inhomogeneity from the frequency separation between the light and dark stripes in narrow fibers Δf_{ea}: it is approximately equal to the whistler frequency. The accuracy of our observations allows us to equate Δf_{ea} and half the frequency separation between the fibers Δf_s (e.g., at frequencies near 24 MHz). For the relative whistler frequency $x = f_w/f_B = 0.01$ (at which the whistlers have the maximum growth rate at moderate loss cone angles ~70°; Kuijpers 1975), we obtain the maximum field strength inside the inhomogeneity, $B \sim 0.9$ G. The plasma β for such a field at a 24-MHz level will be negligible, $\beta \ll 1$, which is expected for the inhomogeneities inside a CME (magnetic cloud).

The whistlers propagate in the propagation direction of the shock front, i.e., in the direction of a decrease in magnetic field and an increase in density (inside the inhomogeneity).

However, the whistler excitation location remains uncertain. It would be natural to assume that the whistlers are excited upstream of the shock front (in background plasma parameters). When the whistlers enter an inhomogeneity with a density enhanced by a factor of 2 or 3, they are trapped into the inhomogeneity region. In this case, the magnetic field changes little (in accordance with the constant parameters of narrow fibers), but the whistlers are scattered by the background plasma, which causes a sharp decrease in x (Chernov 1989). Therefore, the whistler group velocity (Kuijpers 1975)

$$V_{gr} = 2c(f_{Be}/f_{Pe})[x(1-x)^3]^{1/2} \qquad (2)$$

should be $\leq$760 km s^{-1}, for example, for the ratio of the gyrofrequency to the plasma frequency $f_{Be}/f_{Pe} \leq 1/45$ and the relative whistler frequency $x = f_w/f_{Be} \sim 0.0033$ (inside the inhomogeneity). Thus, the whistlers should lag behind the shock front, which is why the narrow fibers have a slower

frequency drift. After about 07:22:40 UT, the narrow fibers became parallel large ones and, hence, the whistlers proved to be standing downstream of the shock front at this time.

The magnetic field can also be determined from the frequency drift of narrow fibers.

According to the formula from Elgaroy (1982) for the model of a doubled Newkirk density at $x = 0.01$, equating the whistler group velocity (2) and the velocity determined from the frequency drift (1), we obtain

$$B = 41.8(\ln f - 1.29)^{-2}|df/dt|. \quad (3)$$

For the frequency $f = 24$ MHz and the drift rate $df/dt = -0.04$ MHz s^{-1}, we obtain $B = 0.47$ G. Thus, it is clear that the density inside inhomogeneities should be approximately doubled in order that Eq. (3) give $B = 0.9$ G determined from the frequency separation.

During their drift, the narrow fibers remain parallel ones (the whistlers are not damped for almost 1.5 min). This is indicative of an almost constant magnetic field strength along the inhomogeneities on scales of ~75 000 km.

A no less complex behavior of the fine structure is observed in type III bursts. Thus, for example, in the type IIIb burst at 07:21:07–10 UT, the entire emission consists of stripes and patches, with the stripes appearing in the spectral segments adjacent to large fibers. Their band width and drift velocity are approximately the same as those for the narrow fibers, which provides evidence for the same whistler–plasma wave interaction mechanism. The pointlike patches are most likely of the same nature, but are short in duration, i.e., the fine structure of the burst results from the passage of a type III beam through a turbulent zone downstream of the shock front.

We cannot see fast bursts in the WIND/WAVE spectra, since the time resolution is limited by 16 s, the time of one scan through the entire frequency range 1–14 MHz (Bougeret et al. 1995). The type II burst consisting of four stripes that form pairwise harmonic structures in the frequency range 0.7–3.5 MHz coincides in time with the overtaking and absorption of the slow CME by the fast one (Fig. 2). These four stripes can be explained by the generation of two shock fronts during the collision of two CMEs. In the left frame of Fig. 4, we see two narrow irregular fronts at the leading CME edge, which are probably these shock fronts.

An additional splitting of broad stripes into narrower ones is observed at frequencies near 2 MHz. Their regular frequency drift breaks down, suggesting a possible contribution from the transition radiation that depends on inhomogeneity parameters inside the CME.

The July 17, 2002 Burst

The general interpretation of the fibers in this event can be the same as that for the August 16, 2002 event. At this time, the shock front was catching up with the CME and the entire fine structure can be associated with the emission from inhomogeneities in the CME tail, including the patchy structure and diffusive bursts. The fibers most likely appear also inside the inhomogeneities. Incidentally, traces of fibers are also seen in the diffuse burst under the second group. The absence of fibers in other diffuse bursts most likely points to different locations of the sources (e.g., along the shock front). The excitation of whistlers is suppressed in these places or, more precisely, the trap for the locked particles does not enclose the entire shock front.

The absence of a strict fiber periodicity may be related to a high (plasma wave) emission level: if the emission frequency depends on intensity, then an additional positive nonlinear addition is added to the emission frequency.

The shorter fiber duration is also difficult to explain by a high intensity. It is determined by the inhomogeneity sizes, which, judging by Fig. 4, can be very different and can have very unusual configurations. The absence of absorption from the low-frequency edge of the fibers is an ordinary property of the fibers in type II bursts. It can be explained by the divergence of fast particles and waves (whistlers) in the space upstream of the shock front (Chernov 1997).

CONCLUSIONS

We analyzed two type II radio bursts in the decametric wavelength range with a fine structure in the form of unusual slowly drifting fibers. For our general analysis of the events we used all the available data in other ranges, in particular, WIND, SOHO, and TRACE data. This provided an insight into the development of flare processes and allowed the possible positions of radio sources to be determined.

Both type II bursts were observed simultaneously at various frequencies of the decametric range with the 1024-channel spectrograph of the UTR-2 radio telescope and the IZMIRAN spectrograph as well as in the WIND/WAVES RAD2 spectra. In contrast to the well-known herringbone structure and patches in the spectrum, this fine structure is distinguished by the formation of narrow-band fibers ($\Delta f_e > 50$–90 kHz at 24 MHz) and is characterized by the possible generation of whistlers between the leading CME edge and the shock front. SOHO/LASCO C2 data were used to analyze the CME. The fiber drift velocity is assumed to be determined by the whistler group velocity inside the

inhomogeneities in the CME tail. Like the continuum modulation in the form of fibers in type IV bursts, the whistlers excited at shock fronts manifest themselves only against the background of enhanced emission from large fibers, which can be the transition radiation from fast particles at inhomogeneities in the CME tail. The unusually low drift velocity of narrow fibers may be determined by the reduction in whistler group velocity inside the inhomogeneities to 760 km s^{-1}. The magnetic field inside the inhomogeneities at a frequency of 24 MHz was ~0.9 G.

ACKNOWLEDGMENTS

This work was supported in part by the Russian Foundation for Basic Research (project no. 05-02-16271) and INTAS-03-5727. We are grateful to M. Kaiser and the WAVES team for the open access to the data at http://lep694.gsfc.nasa.gov/waves/waves.html. We are grateful to the SOHO and TRACE teams for the open access to the databases.

REFERENCES

1. J.-L. Bougeret, M. L. Kaiser, P. J. Kellogg, et al., Space Sci. Rev. **71**, 5 (1995).
2. G. P. Chernov, Astron. Zh. **53**, 1027 (1976) [Sov. Astron. **20**, 582 (1976)].
3. G. P. Chernov, Astron. Zh. **66**, 1258 (1989) [Sov. Astron. **33**, 649 (1989)].
4. G. P. Chernov, Pis'ma Astron. Zh. **23**, 949 (1997) [Astron. Lett. **23**, 827 (1997)].
5. G. P. Chernov, Astron. Zh. **81**, 938 (2004) [Astron. Rep. **48**, 853 (2004)].
6. G. P. Chernov, M. L. Kaiser, J.-L. Bougeret, et al., Sol. Phys. (2006) (in press).
7. O. Elgaroy, *Intermediate Drift Bursts*, Report No. 53 (ITA, Univ. Oslo, 1982).
8. G. D. Fleishman, Pis'ma Astron. Zh. **27**, 296 (2001) [Astron. Lett. **27**, 254 (2001)].
9. V. V. Fomichev, Doctoral Dissertation in Mathematical Physics (IZMIRAN, Moscow, 1986).
10. G. D. Holman and M. E. Pesses, Astrophys. J. **267**, 837 (1983).
11. A. Kruger, *Introduction to Solar Radio Astronomy and Radio Physics* (Reidel, Dordrecht, 1979; Mir, Moscow, 1983).
12. J. Kuijpers, *Collective Wave-Particle Interactions in Solar Type IV Radio Sources* (Utrecht Univ., 1975).
13. J. LaBelle, R. A. Treumann, P. H. Yoon, and M. Karlicky, Astrophys. J. **593**, 1195 (2003).
14. Y. Leblanc, G. A. Dulk, and J.-L. Bougeret, Sol. Phys. **183**, 165 (1998).
15. V. N. Melnik, A. A. Konovalenko, A. A. Stanislavsky, et al., Radiofiz. Radioastron. **9**, 237 (2004).
16. V. N. Melnik, A. A. Konovalenko, V. V. Dorovsky, et al., Sol. Phys. **231**, 143 (2005).
17. G. M. Nita, D. E. Gary, and G. D. Fleishman, Astrophys. J. **629**, L65 (2005).
18. C. Slottje, *Atlas of Fine Structures of Dynamic Spectra of Solar Type IV-dm and Some Type II Radio Bursts* (Utrech Observ., 1981).
19. A. R. Thompson and A. Maxwell, Astrophys. J. **136**, 546 (1962).
20. B. Vršnak, J. Magdalenic, and P. Zlobec, Astron. Astrophys. **413**, 753 (2004).
21. V. V. Zaitsev and V. G. Ledenev, Pis'ma Astron. Zh. **2**, 443 (1976) [Sov. Astron. Lett. **2**, 172 (1976)].

Translated by V. Astakhov